

Select Thy Neighbors: Low Complexity Link Selection for High Precision Cooperative Vehicular Localization

G.M. Hoang^{†‡}, B. Denis[†], J. Härrri[‡], D. T.M. Slock[‡]

[†]CEA-Leti, MINATEC Campus, 17 rue des Martyrs, F38054 Grenoble, Cedex 9, France

[‡]EURECOM, 450 route des Chappes, 06904 Sophia Antipolis, France

E-mails: {giaminh.hoang, benoit.denis}@cea.fr, {jerome.haerri, dirk.slock}@eurecom.fr

Abstract—One major challenge of relying on Dedicated Short Range Communication (DSRC)-equipped vehicles for high precision cooperative localization is related to the high computational complexity and heavy communication loads of exhaustively considering links to all neighbors regardless of their quality. This paper addresses the problem of selecting the best subset of links to spatial neighbors, considering varying degradation first from GPS conditions and second from GPS positioning capabilities. We formulate a computationally efficient particle filter-based link selection algorithms based on Cramér-Rao Lower Bound (CRLB) indicators accounting for neighbors uncertainties. We show that selective fusion significantly reduces the computational complexity and required network traffic with a modest increase in the position error in most cases and an acceptable degradation in the worst-case long-term GPS-denied condition or under severe neighbor positions uncertainties.

I. INTRODUCTION

Geo-localization is a critical requirement of Cooperative Intelligent Transport System (C-ITS) safety and traffic efficiency applications as well as many other applications. The currently proposed C-ITS Basic Set of Applications (BSA) [1] relies on the availability of Global Navigation Satellite System (GNSS), which can provide a positioning precision on the order of 3–10 meters in favorable conditions [2]. This current precision level is obviously not sufficient for Road Hazard Warning (RHW) and most advanced C-ITS applications, such as safety of vulnerable road users or autonomous driving/platooning. The latter would indeed require a sub-meter precision (less than 0.5 m), which is not yet available by any mass market GNSS technology.

In order to improve the localization functionality, connected landmarks can be used by vehicles for relative positioning and multi-lateration [1]. But this approach requires a sufficient number of landmarks forming a specific constellation around a vehicle, which is rarely observable in highly mobile urban conditions. Dedicated Short Range Communication (DSRC) (a.k.a. IEEE 802.11p or ITS-G5) has been rapidly developing to enable wireless communications between vehicles (V2V). Each vehicle periodically broadcasts its GPS-aided estimated position encapsulated in messages called Cooperative Awareness Message (CAMs) or Basic Safety Message (BSM) in EU and US terminology respectively, and which allow neighboring

vehicles to get a cooperative situation awareness of the nearby traffic. These cooperative neighbors, which can be considered as virtual landmarks, may thus contribute to enhance positioning.

In the literature, such cooperative positioning (CP) solutions have already been described to fuse on-board GPS estimates with V2V range measurements relying on the Received Signal Strength Indicator (RSSI) of broadcast CAMs [1]–[3]. However, most of these contributions still assume exhaustive cooperation (i.e., integrating information from all available neighbors) and too optimistic models for input measurements (i.e., in terms of both GPS quality and V2V radio channel conditions). Actually CP performance is strongly affected by the number of neighbors and their geometric configuration while processing and fusing all incoming information. On the other hand integrating fusion-oriented data from numerous neighbors generates high computational complexity and significant overhead (and possibly, extra channel load) at the network level in comparison with more conventional CAM usage. Thus relevant operating trade-offs (e.g., in terms of required number of packets, CAM payload occupancy, refresh rates) must still be found for a better exploitation of the potential of cooperative vehicles, while complying with practical protocol constraints. Regarding the link selection itself, previous works relying on the approximated Cramér-Rao Lower Bound (CRLB) of cooperative position estimates as criterion (e.g., [4], [5] or more recently, [6] in the V2V context) cannot properly account for mobile neighbors uncertainty, whereas more recent Bayesian formulations of such bounds have not yet been applied into the V2V context.

Thus we herein propose new link selection algorithms that aim at more efficient CP procedures under various GPS conditions, by enabling lower footprint with respect to communication means and lower computational complexity. The main related contributions can be summarized as follows: (i) we describe a generic fusion-based CP framework relying on a Particle Filter (PF) that copes with ad hoc communication and positioning characteristics such as distributed and asynchronous position estimates, random CAM transmissions...; (ii) we propose a couple of computationally efficient link selection criteria based on non-Bayesian and Bayesian versions

of the Cramér-Rao Lower Bound (CRLB) characterizing cooperative location estimates (the Bayesian formulation capturing the “ego” and anchors’ uncertainties), in conjunction with a fast sub-optimal closest search (instead of a computationally greedy exhaustive search); (iii) we show that selective CP experiences reduced complexity in terms of both required traffic and computations, while suffering only little precision degradation in most cases including normal operating conditions, harsh and even GPS-denied environments in the short term and even reasonable degradation in very poor or lost GPS signal in the long term, in comparison with exhaustive cooperation schemes; (iv) we point out practical conditions in terms of GPS quality dispersion when the Bayesian CRLB selection criterion would outperform the non-Bayesian criterion, thus opening the floor to context-aware selection and fusion.

The paper is organized as follows. In Section II, we formulate the distributed CP problem in GPS-aided IEEE 802.11p-based VANETs. We then describe a general framework of models and particle filtering strategies dedicated to fusion-based CP in Section III. Next, Section IV addresses the computationally efficient link selection algorithms employing non-Bayesian CRLB and Bayesian CRLB criteria. Simulation results and scenario-based analyses are presented for comparison with more conventional approaches in Section V. Finally, Section VI concludes the paper.

II. GENERAL PROBLEM FORMULATION

We consider here a set of cooperative GPS-equipped vehicles exchanging CAM/BSM over DSRC technology. The goal of an “ego” vehicle is to infer its position (as part of its so-called “state” in the following) based on its own estimated GPS position, on V2V received signal strengths with respect to 1-hop neighbors (measured out of incoming CAMs), and

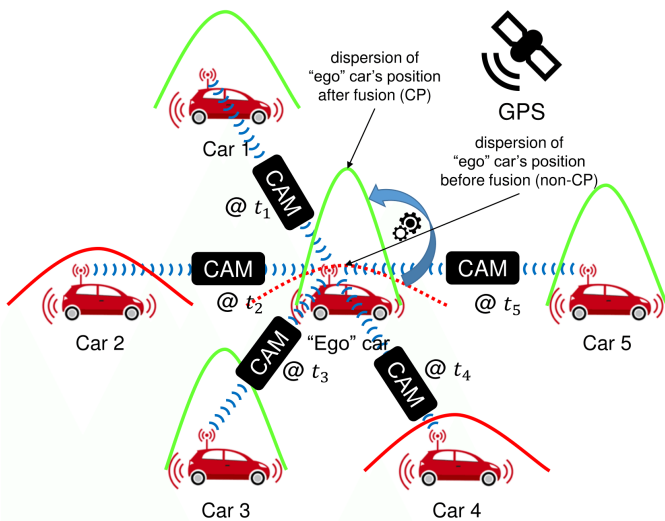


Fig. 1. “Ego” car receiving asynchronous CAMs from 1-Hop “virtual” anchors to perform distributed CP. The dispersion of CP location estimates (i.e. through GPS+DSRC) is expected to be lower than that of non-CP estimates (i.e., standalone GPS).

on imperfect state information from these neighbors, viewed as “virtual” anchors (i.e., estimated locations and their related uncertainties, encapsulated in the CAMs). Fig. 1 illustrates this concept of CP. We do not consider V2I communications here to assist positioning, even though Road Side Units (RSU) could be helpful (e.g., WiFi access points (APs) in most urban environments), as our aim is to remain independent from any additional infrastructure (i.e., other than the V2V communications themselves), not only significantly reducing deployment costs but also operating seamlessly in infrastructure-less roads. However, CP in pure VANETs introduces additional challenges that must be overcome.

First of all, distributed data processing (local position estimation, CAM trigger...) induces event-driven CAM transmissions (and accordingly, RSSI measurements too). Hence on the receiver side, the aggregation of asynchronous data (see Fig. 1) makes the whole information misaligned or outdated and thus useless to CP, unless a careful prediction scheme is employed. Secondly, performing the exhaustive fusion of all the incoming packets from available neighbors is computationally demanding in the location estimation stage (possibly with a varying amount of observations depending on instantaneous connectivity) and maybe not even so informative. Thus selecting the best cooperative links with respect to available neighbors is of primary importance. In addition to decreasing fusion complexity, it would enable to reduce the number of required packets to achieve a given target precision. This would thus contribute to save resources at the network level, either in terms of channel load (e.g., by reducing the refreshment rate of the CP-oriented CAMs) or overhead (under fixed refreshment rates, saving the CAM payloads for other services). However the selection procedure itself shall result on affordable complexity and latency to be useful to future C-ITS applications. In the following, we make tangible proposals to address these different challenges.

III. SYSTEM MODELS AND FILTERING STRATEGIES

The core of any tracking problem is the mobility model to which many different model-based filtering techniques can be applied. Generally, models that are linear in the state dynamics and non-linear in the observations are employed [7]

$$\boldsymbol{\theta}_{i,k+1} = \mathbf{F}_i \boldsymbol{\theta}_{i,k} + \mathbf{f}_{i,k} + \mathbf{G}_i \mathbf{w}_{i,k}, \quad (1a)$$

$$\mathbf{z}_{i,k} = \mathbf{h}(\boldsymbol{\theta}_{i,k}) + \mathbf{n}_{i,k}, \quad (1b)$$

where $\boldsymbol{\theta}_{i,k} = (\mathbf{x}_{i,k}^\dagger, \mathbf{v}_{i,k}^\dagger)^\dagger$ is the true state vector of vehicle i including, for a 2-D system, its position $\mathbf{x}_{i,k} = (x_{i,k}, y_{i,k})^\dagger$ and its velocity $\mathbf{v}_{i,k} = (v_{i,k}^x, v_{i,k}^y)^\dagger$ at time $t_{i,k}$ according to its local estimation timeline¹, \mathbf{F}_i the state transition matrix, \mathbf{f}_i the control inputs (e.g., throttle settings, braking forces), \mathbf{G}_i the matrix that applies the effects of each noise component in the process noise vector $\mathbf{w}_{i,k}$ on the state vector, $\mathbf{h}(\boldsymbol{\theta}_{i,k})$ the transformation matrix that maps the state vector parameters

¹Due to asynchronously sampled time instants, $t_{i,k} \neq t_{j,k}$ if $i \neq j$.

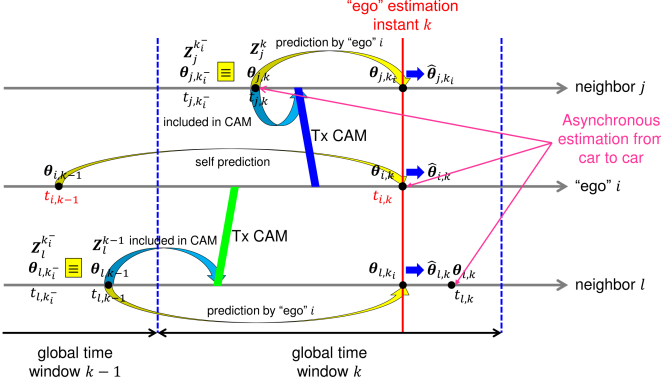


Fig. 2. Example of the space-time schematic managed by the “ego” i whose neighbors are vehicle j and l . Due to asynchronous estimates, the “ego” i needs to perform prediction of received information at its time of interest $t_{i,k}$.

$\theta_{i,k}$ into the measurement/observation $\mathbf{z}_{i,k}$, which is corrupted by a measurement noise term $\mathbf{n}_{i,k}$. Additionally, throughout this paper, we will use the following notations (some of them being also illustrated in Fig. 2)

- θ_{j,k_i} is the true state vector of vehicle j at $t_{i,k}$ according to vehicle i 's estimation timeline (and similarly for $\hat{\mathbf{x}}_{j,k_i}$ and $\hat{\mathbf{v}}_{j,k_i}$). For $j \equiv i$, it means $\theta_{i,k}$ (See Fig. 2);
- θ_{j,k^*} is the true state vector of neighbor j at its latest estimation instant before the “ego” estimation instant k (i.e., $t_{i,k}$), thus it can vary from car to car as shown in Fig. 2. For $i \equiv j$, it means $\theta_{i,k-1}$;
- $\hat{\theta}_{j,k_i}$ is the estimate of θ_{j,k_i} (at time $t_{i,k}$) produced/predicted by the “ego” i depicted in Fig. 2 (and similarly for $\hat{\mathbf{x}}_{j,k_i}$ and $\hat{\mathbf{v}}_{j,k_i}$). For $i \equiv j$, it means $\hat{\theta}_{i,k}$;
- $\mathcal{N}_{i,k:k-1}$ indicates the set of i 's neighbors in its communication range r_{\max} in the time interval $[t_{i,k-1}, t_{i,k}]$;
- $\mathcal{S}_{i,k} \subset \mathcal{N}_{i,k:k-1}$ is the set of car i 's virtual anchors/reference nodes whose CAMs are selected to feed car i 's fusion engine (thanks to link selection...);
- $\theta_{\text{ref},i,k}$ denotes the aggregate state vector of i 's $|\mathcal{S}_{i,k}|$ reference neighbors at fusion time $t_{i,k}$ (thanks to prediction);
- $\mathbf{z}_{i,k}^{\text{GPS}} = (z_{i,k}^x, z_{i,k}^y)^\dagger$ denotes the 2-D GPS position of vehicle i at time $t_{i,k}$;
- $z_{i,k}^{j \rightarrow}$ is the approximated/extrapolated RSSI values² at exact filtering/fusing time $t_{i,k}$ under some circumstances;
- \mathbf{Z}_i^k denotes the set of all vehicle i 's observations up to (and including) time $t_{i,k}$;
- $\mathbf{Z}_j^{k^*}$ is the set of neighbor j 's observations up to (and including) the its latest instant (falling in the window k or $k-1$) before the “ego” estimation instant k (See Fig. 2).

A. The Gauss-Markov Mobility Model

In the vehicular context, we consider a stochastic mobility model, also called modified Gauss-Markov prediction model, since it describes well the correlated velocity of the vehicle as a time-correlated process and makes good prediction of the position and velocity of the vehicle [6]. In discrete time, the

²In practice, due to random/event-driven CAMs, the time at which the RSSI value is read does not necessarily coincide with the filter/fusion time (Fig. 2).

predicted velocity in 2-D is computed based on its previous value and a Gaussian i.i.d process, as follows

$$v_{i,k+1}^{(\cdot)} = \alpha v_{i,k}^{(\cdot)} + (1 - \alpha) \mu_i^{(\cdot)} + \Delta T \sqrt{1 - \alpha^2} w_{i,k}^{(\cdot)}, \quad (2)$$

where (\cdot) can be either x - or y -coordinate, α is the memory level, ΔT the time step, $\mu_i^{(\cdot)}$ the asymptotic 1-D mean velocity, and $a_{i,k}^{(\cdot)} = \sqrt{1 - \alpha^2} w_{i,k}^{(\cdot)}$ the Gaussian i.i.d. 1-D acceleration noise. It is important to remember that vehicles usually move along the lanes on the roads. Intuitively, the uncertainty along the road direction is much higher than that along the dimension orthogonal to the road. If $(\sigma_i^a)^2$ and $(\sigma_i^o)^2$ represent the variances of the uncertainties along and perpendicular to the road respectively, therefore $(\sigma_i^a)^2 \gg (\sigma_i^o)^2$. As a road runs in a direction with an angle Ω counterclockwise from x -axis, a transformation must be applied to account for the bias in the direction, providing information on road geometry within the prediction model (1a) to reduce uncertainty and achieve better predictions. Thus, the process covariance matrix is no longer diagonal, as follows

$$\begin{aligned} \mathbb{E} \left\{ \mathbf{w}_{i,k} \mathbf{w}_{i,k}^\dagger \right\} &= \mathbb{E} \left\{ \begin{pmatrix} w_{i,k}^x w_{i,k}^{x\dagger} & w_{i,k}^x w_{i,k}^{y\dagger} \\ w_{i,k}^y w_{i,k}^{x\dagger} & w_{i,k}^y w_{i,k}^{y\dagger} \end{pmatrix} \right\} \\ &= \begin{pmatrix} \cos \Omega & -\sin \Omega \\ \sin \Omega & \cos \Omega \end{pmatrix} \begin{pmatrix} (\sigma_i^a)^2 & 0 \\ 0 & (\sigma_i^o)^2 \end{pmatrix} \begin{pmatrix} \cos \Omega & -\sin \Omega \\ \sin \Omega & \cos \Omega \end{pmatrix}^\dagger, \end{aligned} \quad (3)$$

where $\mathbf{w}_{i,k} = (w_{i,k}^x, w_{i,k}^y)^\dagger$ denotes 2-D process noise vector.

Recall that the state of vehicle i at its local discrete time k is represented by the vector $\theta_{i,k} = (\mathbf{x}_{i,k}, \mathbf{v}_{i,k})^\dagger$ where $\mathbf{x}_{i,k} = (x_{i,k}, y_{i,k})^\dagger$ and $\mathbf{v}_{i,k} = (v_{i,k}^x, v_{i,k}^y)^\dagger$ are the 2-D position and velocity respectively, the resulting mobility model (1a) yields

$$\begin{aligned} \begin{pmatrix} \mathbf{x}_{i,k+1} \\ \mathbf{v}_{i,k+1} \end{pmatrix} &= \underbrace{\begin{pmatrix} \mathbf{I}_2 & \alpha \Delta T \cdot \mathbf{I}_2 \\ \mathbf{0}_2 & \alpha \cdot \mathbf{I}_2 \end{pmatrix}}_{\mathbf{F}_i(\alpha, \Delta T)} \underbrace{\begin{pmatrix} \mathbf{x}_{i,k} \\ \mathbf{v}_{i,k} \end{pmatrix}}_{\theta_{i,k}} \\ &+ \underbrace{(1 - \alpha) \begin{pmatrix} \Delta T \cdot \mathbf{I}_2 \\ \mathbf{I}_2 \end{pmatrix}}_{\mathbf{f}_i(\alpha, \Delta T)} \underbrace{\mu_i}_{\mathbf{G}_i(\alpha, \Delta T)} + \underbrace{\sqrt{1 - \alpha^2} \begin{pmatrix} \Delta T^2 \cdot \mathbf{I}_2 \\ \Delta T \cdot \mathbf{I}_2 \end{pmatrix}}_{\mathbf{G}_i(\alpha, \Delta T)} \mathbf{w}_{i,k}, \end{aligned} \quad (4)$$

where \mathbf{I}_2 is the identity matrix of size 2.

In the following, we will use this mobility model to perform the predictions of both “ego” and neighbors’ estimated locations and re-synchronize related data before fusion (See step 2 of Algorithm 1).

B. Measurement Model

1) *GPS Absolute Position*: Generally speaking, the 2-D position $\mathbf{x}_{i,k}$ is determined by a GPS receiver and the corresponding measurement $\mathbf{z}_{i,k}^{\text{GPS}}$ is corrupted by additive noise $\mathbf{n}_{i,k}^{\text{GPS}} = (n_{i,k}^x, n_{i,k}^y)^\dagger$, as follows

$$z_{i,k}^x = x_{i,k} + n_{i,k}^x, \quad z_{i,k}^y = y_{i,k} + n_{i,k}^y. \quad (5)$$

For simplicity, the latter errors affecting 2-D coordinates, $n_{i,k}^x$ and $n_{i,k}^y$, are supposed to be independent and identically

distributed (i.i.d) centered Gaussian like in [2], [3], [6].

2) *V2V Received Power*: Received Signal Strength Indicator (RSSI) measurements are directly performed out of the received CAMs, originally used to encapsulate and share geographical awareness information over DSRC channels between vehicles (V2V). The approximated/extrapolated RSSI $z_{i,k}^{j \rightarrow}$ (on a dB scale) at vehicle i at local time $t_{i,k}$ (i.e., while occupying position $\mathbf{x}_{i,k}$) with respect to vehicle j (i.e., occupying position $\mathbf{x}_{j,k}$), is assumed to be measured in Line-Of-Sight (LOS) and to follow the widely used log-distance path loss model³ [8]

$$z_{i,k}^{j \rightarrow} = P(d_0) - 10n_p \log_{10} \left(\frac{\|\mathbf{x}_{i,k} - \mathbf{x}_{j,k}\|}{d_0} \right) + s_{i,k}^{j \rightarrow}, \quad (6)$$

where $P(d_0)$ [dBm] is the averaged received power at a reference distance $d_0 = 1$ m, n_p the path loss exponent, $\|\cdot\|$ the Euclidean distance, and finally $s_{i,k}^{j \rightarrow}$, a shadowing component that is centered Gaussian with standard deviation σ_{Sh} . In the following filtering scheme, observations will be composed of GPS and/or V2V RSSI measurements, depending on the cooperation level.

C. Particle Filter Tracking

As the observation model of interest linking the state vector to the measurements is non-linear here (e.g., See (6)), filtering strategies relying on numerical approximations (e.g., PF) are expected to outperform that based on linear approximations (e.g., Extended Kalman Filters) in terms of accuracy, at the price of higher computational complexity. However, in the vehicular context, the relative extra-cost to supply adequate powerful hardware and software capabilities looks still reasonable (comparing with the cost of the whole car). The key idea of PF is to approximately represent the *a posteriori* density function⁴ by a set of random samples with associated weights and to compute estimates based on these samples and weights [7]. Hence, we approximate the optimal solution by

$$\hat{\boldsymbol{\theta}}_{i,k} \approx \sum_{p=1}^{N_p} w_{i,k}^{(p)} \boldsymbol{\theta}_{i,k}^{(p)}, \quad (7)$$

where $\{\boldsymbol{\theta}_{i,k}^{(p)}\}_{p=1}^{N_p}$ is a set of particles (samples of the state vector) with associated weights $\{w_{i,k}^{(p)}\}_{p=1}^{N_p}$. A classical and intuitive choice for computing these weights involves the likelihood function [7]. We propose to apply the PF described below in Algorithm 1 as the core filter/fusion engine of our CP framework.

³Without loss of generality, we assumed a simplified log-distance model in this work, but the proposed core data fusion engine is not restricted to it. Moreover, detailed measurement campaigns are currently conducted in the frame of the HIGHTS project to provide more sophisticated input models for future evaluations.

⁴In our proof-of-concept validations, CAMs encapsulate the particles cloud to account for local estimates uncertainty, what could result in prohibitive overhead under current standard specifications. This issue, which does not fall in the paper scope, has started been investigated in other works, without contradicting the first findings exposed herein.

Algorithm 1 Bayesian bootstrap (iteration k , “ego” vehicle i)

- 1: receive CAMs from the set $\mathcal{N}_{i,k-1:k}$ of neighboring vehicles, read the RSSI values, and extract the neighboring particle clouds $\boldsymbol{\theta}_{j,k}^{(p)}$, $p = 1 \dots N_p$, $j \in \mathcal{N}_{i,k-1:k}$
- 2: perform prediction/data resynchronization at the “ego” estimation instance k (i.e., the global time $t_{i,k}$)

$$\boldsymbol{\theta}_{j,k_i}^{(p)} \sim p \left(\boldsymbol{\theta}_{j,k_i} \middle| \boldsymbol{\theta}_{j,k}^{(p)} \right), \quad j \in \{i\} \cup \mathcal{N}_{i,k-1:k},$$

$$w_{j,k|k-1}^{(p)} = w_{j,k-1}^{(p)} = 1/N_p, \quad p = 1, \dots, N_p,$$

and build the local dynamic map (LDM) of vehicle i 's neighbors as the first output

$$\hat{\boldsymbol{\theta}}_{j,k_i} \approx \sum_{p=1}^{N_p} w_{j,k|k-1}^{(p)} \boldsymbol{\theta}_{j,k_i}^{(p)} = \frac{1}{N_p} \sum_{p=1}^{N_p} \boldsymbol{\theta}_{j,k_i}^{(p)}, \quad j \in \mathcal{N}_{i,k-1:k}$$

- 3: select the subset $\mathcal{S}_{i,k} \subset \mathcal{N}_{i,k-1:k}$ of the best links
- 4: update new weights according to the likelihood based on (1b)

$$w_{i,k}^{(p)} \propto p \left(\mathbf{z}_{i,k} \middle| \boldsymbol{\theta}_{i,k}^{(p)}, \boldsymbol{\theta}_{\text{ref},i,k}^{(p)} \right), \quad p = 1, \dots, N_p,$$

normalize them to sum to unity, and compute the approximate mean as the second filter/fusion output

$$\hat{\boldsymbol{\theta}}_{i,k} \approx \sum_{p=1}^{N_p} w_{i,k}^{(p)} \boldsymbol{\theta}_{i,k}^{(p)}$$

- 5: perform resampling and broadcast
-

IV. LINK SELECTION

As already mentioned, additional links selection mechanisms must be applied to reduce errors propagation, computational complexity or over-the-air CAM traffic and overhead. We herein set *a priori* the number of selected links to 4 without degrading too significantly the performance [4]–[6], while still considering extra diversity from the minimum number required for non-ambiguous 2-D positioning.

A. Link Selection Criteria

1) *Non-Bayesian Cramér-Rao Lower Bound*: The non-Bayesian CRLB characterizes here the best achievable performance (in the minimum expected mean squared error (MSE) sense) for any non-biased (position) estimator (i.e., conditioned on a given set of reference neighbors). From the positioning point of view, this criterion reflects both the pairwise radio link quality and the geometry of the reference vehicles relative to the “ego” one or Geometric Dilution Of Precision (GDOP). The bound is determined by processing an inverse of the Fisher Information Matrix (FIM) [9], [10]. Consider at the “ego” estimation instant k , $\mathbf{x}_{i,k}$, the position of the “ego” vehicle i and $\{\mathbf{x}_{j,k_i}\}_{j \in \mathcal{S}_{i,k}}$, the positions of its selected reference vehicles, the FIM is defined as

$$\mathbf{J}_{i,k} = \sum_{j \in \mathcal{S}_{i,k}} \mathbb{E}_{\mathcal{S}_{i,k}^{j \rightarrow}} \left\{ -\Delta_{\mathbf{x}_{i,k}}^{\mathbf{x}_{i,k}} \log p \left(z_{i,k}^{j \rightarrow} \middle| \mathbf{x}_{i,k}, \mathbf{x}_{j,k_i} \right) \right\}, \quad (8)$$

where $\Delta_{\mathbf{x}}^{\mathbf{x}} f(\mathbf{x})$ denotes the Laplacian of $f(\mathbf{x})$. Note that as its name suggests, the non-Bayesian CRLB treats both $\mathbf{x}_{i,k}$ and \mathbf{x}_{j,k_i} , $j \in \mathcal{S}_{i,k}$ as deterministic variables even though

they are actually random (i.e., affected by estimation noise). Accordingly, the expectation in (8) is taken with respect to the measurement noise only (i.e., over the shadowing). Under the assumption of centered Gaussian shadowing in (6), the expectation can be computed in closed-form solution [9]

$$\mathbf{J}_{i,k} = \sum_{j \in \mathcal{S}_{i,k}} \frac{1}{\tilde{\sigma}_{\text{Sh}}^2} \frac{(\mathbf{x}_{i,k} - \mathbf{x}_{j,k_i})(\mathbf{x}_{i,k} - \mathbf{x}_{j,k_i})^\dagger}{\|\mathbf{x}_{i,k} - \mathbf{x}_{j,k_i}\|^4}, \quad (9)$$

where $\tilde{\sigma}_{\text{Sh}}^2 = \sigma_{\text{Sh}} \log 10 / (10n_p)$. Nevertheless, neither the true position $\mathbf{x}_{i,k}$ of the ‘‘ego’’ vehicle nor its neighboring positions $\{\mathbf{x}_{j,k_i}\}_{j \in \mathcal{S}_{i,k}}$ are known, thus, the approximate FIM $\hat{\mathbf{J}}_{i,k}$ can be computed with the predicted positions instead i.e., $\hat{\mathbf{x}}_{i,k|k-1}$, $\{\hat{\mathbf{x}}_{j,k_i}\}_{j \in \mathcal{S}_{i,k}}$. Thus, the bound on the location MSE can be expressed in terms of the FIM as follows

$$\text{MSE}(\hat{\mathbf{x}}_{i,k}) \geq \text{tr} \left(\hat{\mathbf{J}}_{i,k}^{-1} \right). \quad (10)$$

This expression shows the expected MSE conditioned on a particular subset $\mathcal{S}_{i,k} \subset \mathcal{N}_{i,k-1:k}$ of neighbors, as the cost function to be minimized by the link selection algorithm.

2) *Bayesian Cramér-Rao Lower Bound*: The Bayesian CRLB (BCRLB) considers the positions as realizations of random variables [4], [10]. Therefore, besides the radio link quality and the geometry of the reference neighbors relative to the ‘‘ego’’ vehicle, this criterion also captures the uncertainties of the ‘‘ego’’ and neighbors’ estimated positions. Assume that at ‘‘ego’’ estimation time epoch k , $\mathbf{x}_{i,k} \sim p(\mathbf{x}_{i,k})$, the position of the ‘‘ego’’ i and $\mathbf{x}_{j,k_i} \sim p(\mathbf{x}_{j,k_i})$, $j \in \mathcal{S}_{i,k}$, the positions of its selected reference vehicles, the Bayesian FIM (BFIM) is now expressed as [11]

$$\mathbf{J}_{i,k}^B = \mathbf{J}_{i,k}^P + \sum_{j \in \mathcal{S}_{i,k}} \left[(\mathbf{J}_{j,k_i}^P)^{-1} + (\mathbf{J}_{j \rightarrow i,k}^M)^{-1} \right]^{-1}, \quad (11)$$

where $\mathbf{J}_{i,k}^P$, \mathbf{J}_{j,k_i}^P are the *a priori* FIMs of the positions of the ‘‘ego’’ i and its reference neighbors $j \in \mathcal{S}_{i,k}$ respectively, while $\mathbf{J}_{j \rightarrow i,k}^M$ denotes the FIM obtained from the link measurement ($j \rightarrow i$). In particular, the prior FIMs are defined as

$$\mathbf{J}_{i,k}^P = \mathbb{E}_{\mathbf{x}_{i,k}} \left\{ -\Delta_{\mathbf{x}_{i,k}}^{\mathbf{x}_{i,k}} \log p(\mathbf{x}_{i,k} | \mathbf{Z}_i^{k-1}) \right\}, \quad (12)$$

and

$$\mathbf{J}_{j,k_i}^P = \mathbb{E}_{\mathbf{x}_{j,k_i}} \left\{ -\Delta_{\mathbf{x}_{j,k_i}}^{\mathbf{x}_{j,k_i}} \log p(\mathbf{x}_{j,k_i} | \mathbf{Z}_j^{k*}) \right\}, \quad (13)$$

where again \mathbf{Z}_i^{k-1} is similar to the previously defined notations and \mathbf{Z}_j^{k*} indicates the set of neighbor j ’s observations before ‘‘ego’’ estimation instant k (i.e., $t_{i,k}$). Assuming $p(\mathbf{x}_{i,k} | \mathbf{Z}_i^{k-1}) \sim \mathcal{N}(\mathbb{E}\{\mathbf{x}_{i,k}\}, \Sigma_{i,k|k-1}^{-1})$ and $p(\mathbf{x}_{j,k_i} | \mathbf{Z}_j^{k*}) \sim \mathcal{N}(\mathbb{E}\{\mathbf{x}_{j,k_i}\}, \Sigma_{j,k_i}^{-1})$ in first approximation, thus $\mathbf{J}_{i,k}^P = \Sigma_{i,k|k-1}^{-1}$ and $\mathbf{J}_{j,k_i}^P = \Sigma_{j,k_i}^{-1}$. On the other hand, the term related to the measurements is now calculated as follows

$$\begin{aligned} \mathbf{J}_{j \rightarrow i,k}^M &= \mathbb{E}_{s_{i,k}^j, \mathbf{x}_{i,k}, \mathbf{x}_{j,k_i}} \left\{ -\Delta_{\mathbf{x}_{i,k}}^{\mathbf{x}_{i,k}} \log p(z_{i,k}^j | \mathbf{x}_{i,k}, \mathbf{x}_{j,k_i}) \right\} \\ &= \frac{1}{\tilde{\sigma}_{\text{Sh}}^2} \mathbb{E}_{\mathbf{x}_{i,k}, \mathbf{x}_{j,k_i}} \left\{ \frac{(\mathbf{x}_{i,k} - \mathbf{x}_{j,k_i})(\mathbf{x}_{i,k} - \mathbf{x}_{j,k_i})^\dagger}{\|\mathbf{x}_{i,k} - \mathbf{x}_{j,k_i}\|^4} \right\}. \end{aligned} \quad (14)$$

Note that the expectation over the measurement noise is performed analytically in (14) still considering the Gaussian shadowing (in dB). Besides, as the expectation with respect to $\mathbf{x}_{i,k}$ and \mathbf{x}_{j,k_i} is tedious to derive analytically, we propose to use numerical integration instead following a Monte Carlo approach. Accordingly, we draw N_p samples $\{\mathbf{x}_{i,k}^{(p)}\}_{p=1}^{N_p}$ and $\{\mathbf{x}_{j,k_i}^{(p)}\}_{p=1}^{N_p}$ from $p(\mathbf{x}_{i,k} | \mathbf{Z}_i^{k-1})$ and $p(\mathbf{x}_{j,k_i} | \mathbf{Z}_j^{k*})$, $j \in \mathcal{S}_{i,k}$ respectively, leading to

$$\begin{aligned} \mathbf{J}_{j \rightarrow i,k}^D &= \frac{1}{\tilde{\sigma}_{\text{Sh}}^2} \int \frac{(\mathbf{x}_{i,k} - \mathbf{x}_{j,k_i})(\mathbf{x}_{i,k} - \mathbf{x}_{j,k_i})^\dagger}{\|\mathbf{x}_{i,k} - \mathbf{x}_{j,k_i}\|^4} p(\mathbf{x}_{i,k} | \mathbf{Z}_i^{k-1}) \\ &\quad \times p(\mathbf{x}_{j,k_i} | \mathbf{Z}_j^{k*}) d\mathbf{x}_{i,k} d\mathbf{x}_{j,k_i} \\ &\approx \frac{1}{\tilde{\sigma}_{\text{Sh}}^2} \frac{1}{N_p} \sum_{p=1}^{N_p} \frac{(\mathbf{x}_{i,k}^{(p)} - \mathbf{x}_{j,k_i}^{(p)})(\mathbf{x}_{i,k}^{(p)} - \mathbf{x}_{j,k_i}^{(p)})^\dagger}{\|\mathbf{x}_{i,k}^{(p)} - \mathbf{x}_{j,k_i}^{(p)}\|^4}. \end{aligned} \quad (15)$$

Finally, similarly to the non-Bayesian CRLB, the final bound on the MSE can be calculated by replacing the FIM $\hat{\mathbf{J}}_{i,k}$ in Equation (10) with the BFIM $\mathbf{J}_{j \rightarrow i,k}^B$. The goal is again to identify the best subset $\mathcal{S}_{i,k} \subset \mathcal{N}_{i,k-1:k}$ that minimizes the conditional positioning MSE.

B. Link Selection Algorithms

In the previous subsection, we have derived the cost functions (in the MSE sense) for the link selection problem. Particularly, considering the ‘‘ego’’ vehicle i at k , given the set $\mathcal{N}_{i,k-1:k}$ of neighboring vehicles, we propose solutions to search for the minimum MSE conditioned on all possible subsets of length S of $\mathcal{N}_{i,k-1:k}$ denoted by $\mathcal{P}_S(\mathcal{N}_{i,k-1:k})$ to find $\mathcal{S}_{i,k}^*$ yielding the best contribution to the CP problem resolution. The optimal link selection would result from an exhaustive search, which is by far too complex in case of high V2V connectivity and thus, not really intended for implementation in a real system. This exhaustive search simply evaluates the cost functions for non-Bayesian or Bayesian CRLBs, for all the possible combinations listed by $\mathcal{P}_S(\mathcal{N}_{i,k-1:k})$. For instance, choosing 4 links out of 10 leads to 210 combinations, what seems still reasonable but 4845 evaluations in case of 20 neighbors appears much more challenging. Therefore, in order to reduce the computational burden, one straightforward approach is to develop a search algorithm that hopefully yields the same solution as that of the exhaustive approach (or at least an equivalent solution). A closer look at the FIMs in both criteria (e.g., in (9) and (14)) reveals that its link-dependent sub-components are inversely proportional to the squared distances between the nodes. Intuitively, this means that performing CP with more distant neighbors leads to suffer from larger MSE or in other heuristic words, the optimal subset of neighbors is expected to be formed among the nearest ones (say, the 8–10 closest neighbors are expected sufficient on most common European highways having 3 lanes). Of course, this intuitive interpretation could be applied with other kinds of V2V metrics but it is all the more noticeable within RSSI-

based CP due to the considered log-normal path loss model, thus making the closest search even more relevant. The overall selection algorithms are summarized in Algorithm 2.

Algorithm 2 Sup-optimal closest search of S most informative links among C most potential ones (iteration k , “ego” car i)

```

1: if  $|\mathcal{N}_{i,k-1:k}| > C$  then
2:   estimate  $\hat{d}_{j \rightarrow i,k} = \|\hat{\mathbf{x}}_{j,k_i} - \hat{\mathbf{x}}_{i,k}\|$  w.r.t.  $j \in \mathcal{N}_{i,k-1:k}$ 
3:   sort the set  $\{\hat{d}_{j \rightarrow i,k}\}_{j \in \mathcal{N}_{i,k-1:k}}$ 
4:   get  $C$  nearest neighbors from  $\mathcal{N}_{i,k-1:k}$  to build  $\mathcal{C}_{i,k}$ 
5: else
6:    $\mathcal{C}_{i,k} = \mathcal{N}_{i,k-1:k}$ 
7: end if
8: if  $|\mathcal{C}_{i,k}| > S$  then
9:   create the set  $\mathcal{P}_S(\mathcal{C}_{i,k})$  of all subsets of  $\mathcal{C}_{i,k}$  of size  $S$ 
10:  for  $s = 1$  to  $|\mathcal{P}_S(\mathcal{C}_{i,k})|$  do ▷ subset index
11:    let  $\mathcal{P}_S(\mathcal{C}_{i,k})[s]$  be the  $s$ -th subset in  $\mathcal{P}_S(\mathcal{C}_{i,k})$ 
12:    determine the bound on the MSE

```

$$\text{MMSE}(\hat{\mathbf{x}}_{i,k})[s] = \begin{cases} \text{tr} \left\{ \left(\hat{\mathbf{J}}_{i,k}[s] \right)^{-1} \right\}, & \text{if non-Bayes} \\ \text{tr} \left\{ \left(\mathbf{J}_{i,k}^B[s] \right)^{-1} \right\}, & \text{if Bayes} \end{cases}$$

where $\hat{\mathbf{J}}_{i,k}[s], \mathbf{J}_{i,k}^B[s]$ are with the set $\mathcal{P}_S(\mathcal{C}_{i,k})[s]$

```

13: end for
14: select the best subset  $s^* = \arg \min_s \{\text{MMSE}(\hat{\mathbf{x}}_{i,k})[s]\}$ 
15:  $\mathcal{S}_{i,k}^* = \mathcal{P}_S(\mathcal{C}_{i,k})[s^*]$ 
16: else
17:    $\mathcal{S}_{i,k}^* = \mathcal{C}_{i,k}$ 
18: end if

```

V. POSITIONING EVALUATION

A. Simulation Settings and Scenarios

In our MATLAB-based evaluation framework, we model a 3-lane urban highway where 15 802.11p-connected cars are driving (in the same direction) at the average speed of 110 km/h (i.e., ≈ 30 m/s). The random CAM generation time between the instant at which CAM generation is triggered (GPS position is sampled) and the instant at which the message is delivered to the transport layer is uniformly drawn in the interval $[0, 50]$ ms (complying with [12]). Table I summarizes the other important parameters used for our simulations.

TABLE I
OTHER IMPORTANT SIMULATION PARAMETERS.

Mobility model α	Gauss-Markov mobility model
Memory level α	0.95
Sampling period ΔT	0.1 [s]
GPS/CAM rate	10 [Hz] (critical) [12]
CAM generation time	$\mathcal{U}(0, 50)$ [ms] (complying with [12])
Path loss exponent n_p	1.9 (V2V in highways) [8]
Std. of shadowing σ_{Sh}	2.5 [dB] (V2V in highways) [8]
Number of particles	500

In the first evaluation scenario (S1), we consider vehicles traveling through an urban canyon (see Fig. 3). GPS estimates at each vehicle are affected by varying standard deviations (SD) with large spatial correlation as depicted in

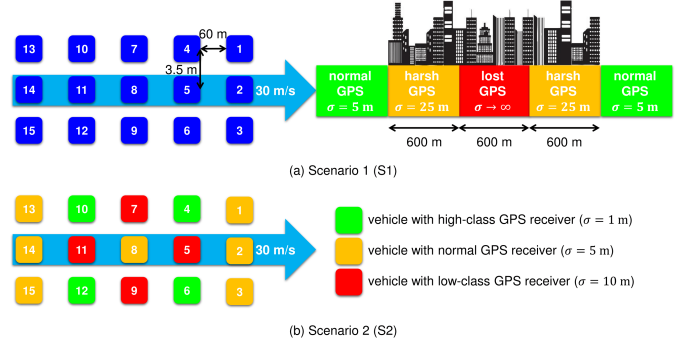


Fig. 3. Topology of the evaluated VANET and associated configurations for S1 (urban canyon) and S2 (different classes of GPS receiver).

Fig. 3(a) whereas the V2V RSSI-based measurement quality is assumed to remain unchanged. Four different positioning schemes are then compared in terms of accuracy and service continuity i.e., stand-alone filtered GPS, exhaustive CP, CRLB-based selective CP, and BCRLB-based selective CP.

In the second evaluation scenario (S2), we consider a heterogeneous configuration where vehicles have the same visibility to satellites, but suffer from disperse and independent GPS precision levels due to different receiver capabilities (e.g., high-class or basic receivers) as illustrated in Fig. 3(b).

These two scenarios are complementary and cumulative, as S1 describes the degradation from GPS signals, whereas S2 considers the degradation from GPS receiver capabilities, both being common in real conditions.

B. Results

1) *Testing Scenario 1 (S1)*: Figure 4 shows the root mean square error (RMSE) of the position estimates of all vehicles as a function of time. Note that the 15 vehicles need approximately 8 s to completely enter/leave the different areas (due to its length of $60 \times 4 = 240$ m and speed of about 30 m/s) causing some transitions in GPS precision levels, as depicted on the same figure. As expected, the CP outperforms the non-CP (i.e., stand-alone filtered GPS) in terms of accuracy and service continuity (i.e., preventing the error from flourishing in harsh/lost conditions). In favorable GPS conditions, the gains yielded by CP over non-CP are modest (relative drop in RMSE of about 9% by exhaustive CP and no drop by selective approaches) whereas in harsh or lost GPS environments, huge improvements in accuracy are observed. In particular, in comparison with non-CP, a relative fall in RMSE of 33% is experienced by exhaustive CP and of about 21% by both selective schemes in harsh areas whereas in GPS-denied periods, relative drops of 30% and of 21% are reported respectively. The reason can be understood as follows: in comparison with the GPS position, RSSI measurements to virtual anchors can contribute to the positioning performance but in a modest way due to the non-linear relationship between received power and state (derived from the distance to the known virtual anchor), the virtual anchors' uncertainties and GDOP, the extrapolated/approximate RSSI values at fusion time, the RSSI shadowing dispersion, etc. In other words,

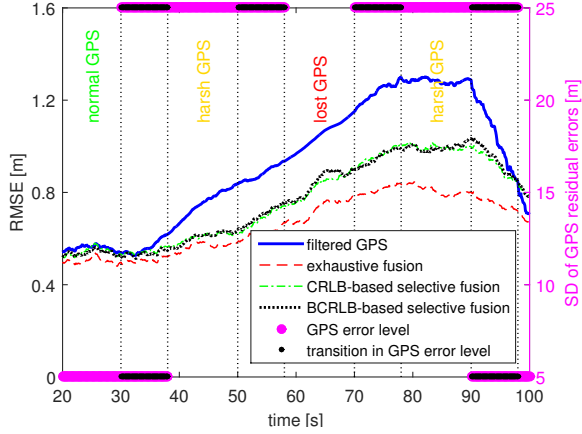


Fig. 4. Localization RMSE (over vehicles) as a function of time when GPS quality varies depending on the geographic area (S1).

when the accuracy of the filtered GPS remains high enough, there is little room for improvement by fusing with DSRC and vice versa, when GPS performance is degraded, the accuracy gain through DSRC is more noticeable.

Quantitatively, both CRLB and BCRLB-based selective fusion schemes are quasi equivalent, and suffer both from a RMSE increase of 10%, 18%, and 14% in normal, harsh, and lost GPS respectively in comparison with exhaustive CP due to the information loss. Note that in our scenario, the positioning error in harsh GPS conditions is superior than that in lost GPS. This is not really contradictory since the “harsh” zone is composed of 2 distinct areas (See again Fig. 3) and the latter (i.e., that after the “lost” period) is more severe due to errors accumulation during the “lost” interval (i.e., reflecting the memory effect pointed out in [3]). From the communication point of view, selective CP dramatically reduces the number of required packets (more than 70% shown in Fig. 5) considering an error increase of 14–18% in worst cases and of 10% in normal cases. Last but not least, from the processing and fusing points of view, the complexity of the particle-based core engine is mainly related to the weights update (See line 4 in Algorithm 1). Particularly, the complexity scales as $\mathcal{O}(N_p |\mathcal{S}_{i,k}|)$ where the number of particles N_p can be large (typically 500–5000). In our scenario, without link selection, $|\mathcal{S}_{i,k}| = 14$, whereas with link selection $|\mathcal{S}_{i,k}| \leq 4$.

In summary, link selection is critical to significantly reduce the computational complexity as well as the network traffic without losing significant accuracy. In this specific scenario, the BCRLB (i.e. by design more adapted to heterogeneous GPS conditions) can just match as expected the CRLB.

2) *Testing Scenario 2 (S2)*: While matching the classic CRLB in scenarios considering homogeneous neighboring vehicles uncertainties (as in scenario S1), the BCRLB criterion shows its efficiency when considering more realistic heterogeneous large dispersion of neighboring vehicles uncertainties. Considering our illustrative example, one can classify vehicles into four classes of dispersion: (i) full topology (i.e., cars fully surrounded by neighbors) vs. partial topology (i.e., cars on

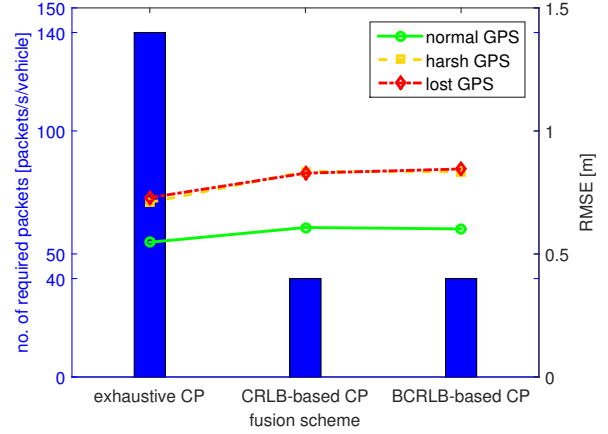


Fig. 5. Trade-off between the number of required packets for CP and the localization RMSE (over vehicles and time) in different GPS conditions (S1).

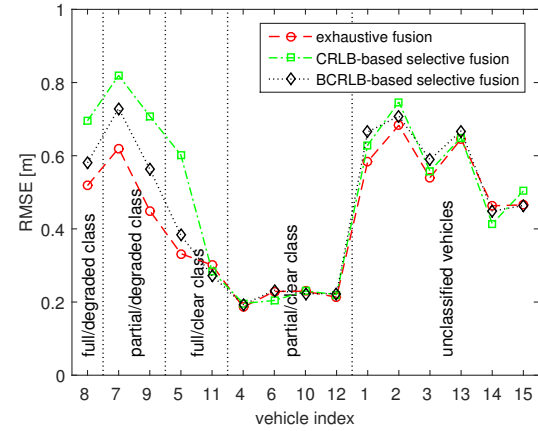


Fig. 6. Localization RMSE (over the full trajectory) of different fusion schemes at each vehicle (S2).

outside lanes); and (ii) clear GPS (i.e., cars whose nearest neighbors have good GPS/estimates) vs. degraded GPS (i.e., cars whose closest neighbors have poor GPS/estimates), as reported in Table II (the remaining are not classified due to strong border effects).

TABLE II
CLASSIFICATION OF VEHICLES W.R.T THE UNCERTAINTY DISPERSION.

Criterion	Full topology	Partial topology
Clear GPS	5, 11	4, 6, 10, 12
Degraded GPS	8	7, 9

Fig. 6 shows the positioning performance in terms of RMSE (over the full trajectory) for each vehicle whereas Fig. 7 demonstrates the empirical cumulative distribution functions (CDFs) for one representative vehicle of each class. Both confirm that in 2 degraded classes when the nearest neighbors experience poor GPS positions or estimates, the classic CRLB criterion neglecting the anchor uncertainties fails to capture the optimal set of neighbors (See the two top sub plots in Fig. 7). In other words, the strong dependency of RSSI measurements onto distances to the neighbors in the

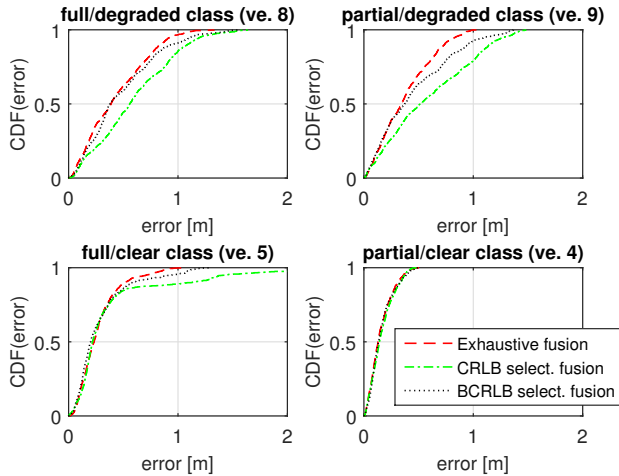


Fig. 7. CDF of localization errors for different fusion schemes at 4 representative vehicles with distinct GPS quality classes (S2).

FIM tricks the CRLB to choose among a small subset of the nearest candidates, regardless of their dispersion. As expected, in the 2 clear classes when the nearest neighbors have good GPS or estimates, the selections are likely to be very similar leading to equivalent performance (See the two bottom sub plots in Fig. 7).

In brief, the second scenario accounts for more realistic heterogeneous conditions (at a smaller scale), where the proposed BCRLB solution would be definitely more helpful.

C. Preliminary Cooperative Application Impact

Although a larger application evaluation is left to future work, we confront here the link selection performance with tangible application needs. Considering the Highway Capacity Manual (HCM) recommendation of a 2-second time between two successive vehicle in free flow traffic, a typical cooperative traffic safety application would need to have a clear position awareness corresponding to at least the distance between two successive vehicles. This translates to about 30 m and 60 m inter-distance considering a speed of 50 km/h in urban and 100 km/h on highways respectively. In the worst case, exhaustive CP yields an error of about 0.85 m (See Fig. 4). Even while losing 14–18% of accuracy through selective fusion, one would still get relative longitudinal error of 1.6% (resp. 3%) at 60 m (resp. 30 m)⁵, and a fully acceptable increased error of 0.2% between an exhaustive and selective fusion.

VI. CONCLUSION AND FUTURE WORK

This paper contributes to solve the selective fusion problem of cooperative vehicular localization where performing exhaustive scheme is questionable due to heavy required communication traffic and computational processing. Both classic non-Bayesian and Bayesian CRLB criteria are thoroughly investigated and incorporated in a computationally efficient search algorithm to reach the subset of the most informative

neighbors so as to minimize the performance degradation causing by information loss. These proposed are evaluated in many realistic environments and in different network settings using a generic fusion-based CP framework for vehicular context. We have found that: (i) it is worthy of employing selective fusion in vehicular CP owing to the aforementioned benefits; (ii) the dispersion of “virtual” anchor uncertainties should be monitored to prevent from having wrong cooperative neighbors in some special but common situations. Future works shall investigate the triggering conditions and criteria to adaptively switch between different selective fusion schemes (including exhaustive fusion), thus leading to more efficient context-aware data fusion. More sophisticated propagation channel assumptions may be incorporated in the studies as well to capture real-world effects on both link selection and positioning in practical environments and scenarios.

ACKNOWLEDGMENT

This work has been performed in the frame of the *HIGHTS* project, which is funded by the European Commission (636537-H2020).

EURECOM acknowledges the support of its industrial members, namely, BMW Group Research and Technology, IABG, Monaco Telecom, Orange, SAP, ST Microelectronics, and Symantec.

REFERENCES

- [1] A. Boukerche, H. A. Oliveira, E. F. Nakamura, and A. A. Loureiro, “Vehicular ad hoc networks: A new challenge for localization-based systems,” *Computer Communications*, vol. 31, no. 12, pp. 2838 – 2849, 2008. Mobility Protocols for ITS/VANET.
- [2] R. Parker and S. Valaee, “Vehicular node localization using received-signal-strength indicator,” *IEEE Trans. on Veh. Tech.*, vol. 56, pp. 3371–3380, Nov. 2007.
- [3] N. Drawil and O. Basir, “Intervehicle-communication-assisted localization,” *IEEE Trans. on Intel. Transp. Syst.*, vol. 11, pp. 678–691, Sept. 2010.
- [4] K. Das and H. Wymeersch, “Censoring for bayesian cooperative positioning in dense wireless networks,” *IEEE JSAC*, vol. 30, pp. 1835–1842, Oct. 2012.
- [5] S. Zirari and B. Denis, “Velocity-based CRLB predictions for enhanced cooperative links selection in location-enabled mobile heterogeneous networks,” in *Proc. WPNC’13*, pp. 1–6, Mar. 2013.
- [6] G. M. Hoang, B. Denis, J. Härrä, and D. T. Slock, “Distributed link selection and data fusion for cooperative positioning in GPS-aided IEEE 802.11p VANETs,” in *Proc. WPNC’15*, Mar. 2015.
- [7] F. Gustafsson, F. Gunnarsson, N. Bergman, U. Forssell, J. Jansson, R. Karlsson, and P.-J. Nordlund, “Particle filters for positioning, navigation, and tracking,” *IEEE Trans. on Sig. Proc.*, vol. 50, pp. 425–437, Feb. 2002.
- [8] L. Cheng, B. Henty, D. Stancil, F. Bai, and P. Mudalige, “Mobile vehicle-to-vehicle narrow-band channel measurement and characterization of the 5.9 GHz Dedicated Short Range Communication (DSRC) frequency band,” *IEEE JSAC*, vol. 25, pp. 1501–1516, Oct. 2007.
- [9] N. Patwari, A. Hero, M. Perkins, N. Correal, and R. O’Dea, “Relative location estimation in wireless sensor networks,” *IEEE Trans. on Sig. Proc.*, vol. 51, pp. 2137–2148, Aug. 2003.
- [10] H. L. V. Trees and K. L. Bell, *Bayesian Bounds for Parameter Estimation and Nonlinear Filtering/Tracking*. Wiley-IEEE Press, 2007.
- [11] S. Van de Velde, G. Abreu, and H. Steendam, “Bayesian CRLB for hybrid ToA and DoA based wireless localization with anchor uncertainty,” in *Proc. IEEE WPNC’15*, p. 5, 2015.
- [12] “Intelligent transport systems (ITS); Vehicular Communications; Basic Set of Applications; Part 2: Specification of Cooperative Awareness Basic Service,” *ETSI Std. EN 302 637-2 V1.3.2*, Oct. 2014.

⁵Lateral errors yet remain high regardless of the strategy.